

STRESS-STRAIN STATE OF PARALLEL CYLINDRICAL TUBES FILLED WITH LIQUID UNDER HARMONIC LOADS

B.S. Raxmonov

Prof. DSc, Urgench State University named after Abu Rayhan Beruni.

U.I. Safarov

Dots. PhD, Tashkent Institute of Architecture and Civil Engineering.

<https://doi.org/10.5281/zenodo.18033085>

Abstract. The study examines the stress–strain state of parallel cylindrical tubes filled with liquid. The problem is solved in a bicylindrical coordinate system under the action of harmonic waves. An analytical solution is obtained in terms of special Bessel and Hankel functions, along with numerical results. A parametric analysis of the dynamic stress coefficient is carried out.

Keywords: cylindrical tube, liquid, harmonic waves, bicylindrical coordinate system, special functions.

Some Fundamental Relations of the Theory of Elasticity. This section presents several basic equations of the theory of elasticity in curvilinear coordinates. It is known that, according to the static theory of elasticity, the Lamé equation in vector form has the following form [1, 2, 3]:

$$(\lambda + 2\mu) \operatorname{grad} \operatorname{div} \vec{u} - \mu \operatorname{rot} \operatorname{rot} \vec{u} + Q \vec{f} = 0 \quad (1)$$

where λ and μ are the Lamé coefficients, defined by the formulas:

$$\lambda = \frac{\nu E}{(1 - 2\nu)(1 + \nu)}, \quad \mu = \frac{E}{2(1 + \nu)}, \quad \vec{u} - \text{displacement vector}, \quad Q \vec{f} - \text{vector}$$

of body forces. The operators appearing in equation (1) for a right-handed system of curvilinear orthogonal coordinates are defined as follows:

$$\begin{aligned} \operatorname{grad} \phi &= \frac{1}{\sqrt{q_{11}}} \frac{\partial \phi}{\partial \alpha_1} \vec{i}_1 + \frac{1}{\sqrt{q_{22}}} \frac{\partial \phi}{\partial \alpha_2} \vec{i}_2 + \frac{1}{\sqrt{q_{33}}} \frac{\partial \phi}{\partial \alpha_3} \vec{i}_3, \quad \operatorname{rot} \vec{u} = \frac{1}{\sqrt{q}} \mathbf{G} \\ \operatorname{div} \vec{u} &= \frac{1}{\sqrt{q}} \left[\frac{\partial}{\partial \alpha_1} \left(u_1 \sqrt{\frac{q}{q_{11}}} \right) + \frac{\partial}{\partial \alpha_2} \left(u_2 \sqrt{\frac{q}{q_{22}}} \right) + \frac{\partial}{\partial \alpha_3} \left(u_3 \sqrt{\frac{q}{q_{33}}} \right) \right] \\ \mathbf{G} &= \begin{vmatrix} \sqrt{q_{11}} \vec{i}_1 & \sqrt{q_{22}} \vec{i}_2 & \sqrt{q_{33}} \vec{i}_3 \\ \frac{\partial}{\partial \alpha_1} & \frac{\partial}{\partial \alpha_2} & \frac{\partial}{\partial \alpha_3} \\ u_1 \sqrt{q_{11}} & u_2 \sqrt{q_{22}} & u_3 \sqrt{q_{33}} \end{vmatrix} \end{aligned}$$

where α_i - are the curvilinear coordinates ($i = 1 \dots 3$), q_{ij} — components of the metric tensor, defined by the formula:

$$q_{ij} = \sum_{k=1}^3 \frac{\partial x_k}{\partial \alpha_i} \frac{\partial x_k}{\partial \alpha_j}$$

x_k — Cartesian coordinates ($k = 1 \dots 3$), q — the square of the Jacobian determinant of the transformation from the Cartesian coordinate system to the curvilinear coordinate system.

For orthogonal curvilinear coordinates only the diagonal components of the metric tensor q_{ij} - are nonzero. In this case, $q = \sqrt{\prod_{i=1}^3 q_{ii}}$, and the fundamental differential quadratic form is given by the formula: $ds^2 = \sum_{i=1}^3 q_{ii} d\alpha_i^2$. To determine the stress state of the soil and to formulate mixed boundary conditions, it is necessary to use relations that express stress in terms of displacement. We employ the geometric equations derived by Novitsky V.

$$\varepsilon_{ii} = \frac{\partial}{\partial \alpha_i} \left(\frac{u_i}{h_i} \right) + \frac{1}{2h_i^2} \sum_{j=1}^3 \frac{\partial h_i^2}{\partial \alpha_j} \frac{u_j}{h_j} \quad (2)$$
$$\varepsilon_{ij} = \frac{1}{2h_i h_j} \left[h_i^2 \frac{\partial}{\partial \alpha_i} \left(\frac{u_j}{h_j} \right) + h_j^2 \frac{\partial}{\partial \alpha_j} \left(\frac{u_i}{h_i} \right) \right] \quad i \neq j, \quad j = \overline{1,3}$$

In addition, we use the constitutive equation (Hooke's law) [2].

$$\sigma_{ij} = \lambda \delta_{ij} \sum_{k=1}^3 \varepsilon_{kk} + 2\mu \varepsilon_{ij} \quad (3)$$

Substituting (2) into (3), we obtain:

$$\sigma_{ij} = \lambda \sum_{k=1}^3 \left[\frac{\partial}{\partial \alpha_k} \frac{u_k}{h_k} + \frac{1}{2h_k^2} \sum_{j=1}^3 \frac{\partial h_k^2}{\partial \alpha_j} \frac{u_j}{h_j} \right] + 2\mu \left[\frac{\partial}{\partial \alpha_i} \frac{u_i}{h_i} + \frac{1}{2h_i^2} \sum_{j=1}^3 \frac{\partial h_i^2}{\partial \alpha_j} \frac{u_j}{h_j} \right] \quad (4a)$$

$$\sigma_{ij} = \frac{\mu}{h_i h_j} \left[h_i^2 \frac{\partial}{\partial \alpha_i} \frac{u_j}{h_j} + h_j^2 \frac{\partial}{\partial \alpha_j} \frac{u_i}{h_i} \right], \quad i \neq j \quad (4b)$$

where $h_i^2 = q_{ii}$. Now we formulate the linear elasticity problem for the computational models in cylindrical coordinates r, θ and z . We use the components of the displacement vector u_r, u_θ and u_z as the unknowns. The cylindrical coordinate system is related to the Cartesian coordinate system by the following relations:

$$x = r \cos \theta; \quad y = r \sin \theta, \quad z = z, \quad ds^2 = dr^2 + r^2 d\theta^2 + dz^2. \quad (5)$$

Using formula (5), we obtain

$$h_1^2 = h_3^2 = q_{11} = q_{33} = 1, \quad h_{22}^2 = q_{22} = r^2$$

As the coordinates α_i ($i = 1, 3$), we use:

$$\alpha_1 = r, \quad \alpha_2 = \theta, \quad \alpha_3 = z \quad (6)$$

Substituting (5) and (6) into (1), and then substituting the resulting expression into formula (4) and taking into account the above, we obtain the following system of Lamé equations in cylindrical coordinates:

$$\begin{aligned} & (\lambda + 2\mu)(u_r)_{rr} + \frac{\mu_2}{r}(u_r)_{\theta\theta} + \mu(u_z)_{zz} + \frac{\lambda + \mu}{r}(u_\theta)_{\theta r} + (\lambda + \mu)(u_z)_{zz} + \\ & + \frac{\lambda + 2\mu}{r}(u_r)_r - \frac{\lambda + 3\mu}{r^2}(u_\theta)_\theta - \frac{\lambda + 2\mu}{r^r}u_r = 0, \\ & \mu(u_\theta)_{zz} + \frac{\lambda + 2\mu}{r^2}(u_\theta)_\theta + \mu(u_\theta)_{zz} + \frac{\lambda + \mu}{r}(u_r)_{r\theta} + \frac{\lambda + \mu}{r}(u_z)_{z\theta} + \\ & + \frac{\mu}{r^2}(u_r)_\theta - \frac{\mu}{r}u_\theta = 0, \\ & \mu(u_z)_{rr} + \frac{\mu}{r^2}(u_\theta)_{\theta\theta} + (\lambda + 2\mu)(u_z)_{zz} + (\lambda + \mu)(u_r)_{rr} + \\ & + \frac{\lambda + \mu}{r}(u_\theta)_{\theta z} + \frac{\lambda + \mu}{r}(u_r)_z = 0 \end{aligned} \quad (7)$$

where the indices r , θ and z outside the brackets denote partial derivatives with respect to the corresponding coordinates. The boundary conditions on the outer surface of the pipe correspond to the condition of perfect contact with the soil, while the inner surface is free:

$$\begin{aligned} r = R : u_{r1} &= u_{r2}, u_{\theta1} = u_{\theta2}, u_z = u_{z2}, \\ \sigma_{rr1} &= \sigma_{rr2}, \sigma_{r\theta1} = \sigma_{r\theta2}, \sigma_{rz1} = \sigma_{rz2}, \\ r = R_0 : \sigma_{rr2} &= 0, \sigma_{r\theta1} = 0, \sigma_{rz1} = 0, \end{aligned} \quad (8)$$

where the indices '1' and '2' denote, respectively, the materials of the surrounding medium and the pipe. The boundary conditions that ensure the equality of the normal components of the velocities of the fluid and the shell are

$$(\vec{V} \cdot \vec{n}) \Big|_{r=a} = + \frac{a_{r2}}{a} \quad (9)$$

where \vec{V} - the velocity of a fluid particle; n - is the normal to the surface at $r = a$, w - is the radial displacement of the shell. To fully close the problem formulation, it is necessary to supplement conditions (8) and (9) with the conditions at infinity. $\mathbf{u} \rightarrow \mathbf{0}$.

$$\text{At } \mathbf{R} = \sqrt{x^2 + y^2 + z^2} \rightarrow \infty \quad (10)$$

supplemented by certain radiation conditions.

For non-stationary problems, the radiation conditions require the fulfillment of the causality principle, and the medium must exhibit no displacements outside the region bounded by the leading front of the waves generated by the vibration sources.

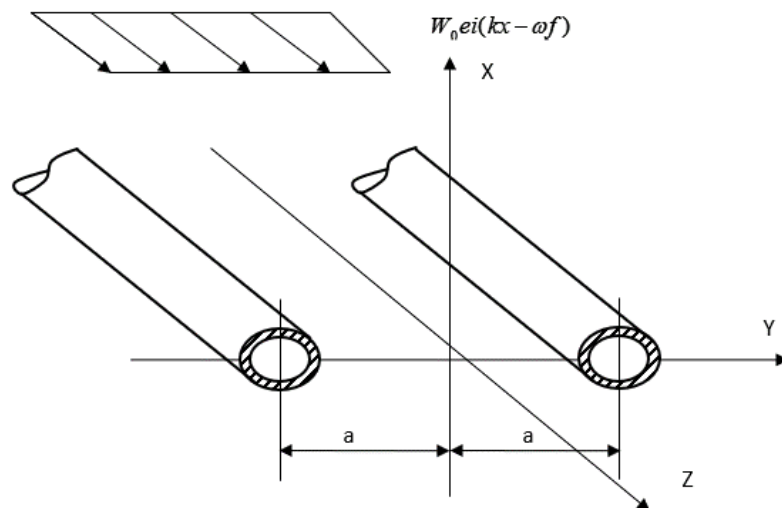


Figure 1. Computational scheme.

Consider the problem of the dynamic theory of linear elasticity concerning the effect of seismic waves on pipes laid in a high embankment in two parallel lines and filled with an ideal compressible fluid. We consider the case when the incident wave strikes perpendicular to the axis connecting the centers of the pipes and also perpendicular to the longitudinal axes of those pipes.

The computational model is shown in Figure 1. The bicylindrical coordinate system is related to the Cartesian coordinate system by the following relations:

$$x = (a \sin \xi) / (ch \eta - \cos \xi), \quad y = (a \sinh \eta) / (ch \eta \cos \xi), \quad z = z \quad (11)$$

where a is half the distance between the points $\eta = -\infty$ and $\eta = \infty$.

Then, substituting (11) into (5, 6), and substituting the resulting expressions into (6), we obtain the following form:

$$ds^2 = a^2 (ch \eta - \cos \xi)^{-2} d\xi^2 + a^2 (ch \eta - \cos \xi)^{-2} d\eta^2 + dz^2 \quad (12)$$

Using formula (11), we obtain

$$h_1^2 = h_2^2 = q_{11} = q_{22} = a^2 (ch \eta - \cos \xi)^{-2}, \quad h_3^2 = q_{33} = 1 \quad (13)$$

Assuming that $\alpha_1 = \xi$, $\alpha_2 = \eta$, $\alpha_3 = z$, and substituting (12) and (13) into (1) - (11), and taking into account that the problem is planar, we obtain the following Helmholtz equation in bipolar coordinates:

$$[a^{-2} (ch \eta - \cos \xi)^2] [(\nabla)_{\xi\xi} + (\nabla)_{\eta\eta}] + k^2 v = 0 \quad (14)$$

where

$$\frac{\sin \xi}{ch \eta - \cos \xi} = \begin{cases} 2 \sum_{n=1}^{\infty} e^{-n\eta} \sin n\xi & \eta > 0 \\ 2 \sum_{n=1}^{\infty} e^{n\eta} \sin n\xi & \eta < 0 \end{cases} \quad (15)$$

Equation (14), after some transformations, reduces to the form

$$(\nabla)_{\xi\xi} + (\nabla)_{\eta\eta} + (2kae^{\pm\eta})^2 v = 0 \quad (16)$$

We will seek the solution of equation (14) in the form of a series:

$$v = \sum_{n=0}^{\infty} [v_n^a(\eta) \cos n\xi + v_n^b(\eta) \sin n\xi] e^{-i\omega t} \quad (17)$$

Substituting (17) into (16) and equating the coefficients of the corresponding harmonics, we obtain the following ordinary differential equation:

$$v_n'' + [(2kae^{\pm\eta})^2 - n^2]v_n = 0 \quad (18)$$

By the standard substitution

$$v_n(\eta) = z(t), \quad t = \exp(\pm\eta)$$

we reduce (18) to a Bessel equation of the form

$$t^2 z'' + tz' + (4k^2 a^2 - n^2)z = 0 \quad (19)$$

which has a particular solution in the form of the cylindrical function

$Z(2ake^{\mp\eta})$, and the solution of the Helmholtz equation takes the following form:

$$\begin{aligned} \varphi &= \sum_{n=0}^{\infty} A_n Z_n(2ake^{\mp\eta}) \cos n\xi e^{-i\omega t} \\ \psi &= \sum_{n=0}^{\infty} B_n Z_n(2ake^{\mp\eta}) \sin n\xi e^{-i\omega t} \end{aligned} \quad (20)$$

Now we impose the boundary conditions. For this we use condition (20) and the substitution $r = \eta$ and $\theta = \xi$. Taking into account the obtained relations, we will seek the solution of the boundary-value problem for the case when a P-wave (compressional) and an SV-wave (shear), incident perpendicular to the y-axis, strike the two underground pipes. The wave potential is given by:

$$\varphi^{(i)} = A e^{i\alpha x - i\omega t} \quad (21)$$

To express equation (21) in the form of equation (20), we rewrite (21) using (12) in bipolar cylindrical coordinates.

$$\varphi_1^{(i)} = A e^{ik2a \exp(\mp)\eta \sin \xi e^{-i\omega t}} \quad (22)$$

By expanding the second factor of expression (22) into a Fourier series (in complex form) and performing some minor transformations, we obtain the final expression for the potential of the incident P-wave:

$$\varphi_1^{(i)} = A \sum_{n=0}^{\infty} \varepsilon_n J_n(\alpha_1 \tau) \cos n\xi e^{-i\omega t} \quad (23)$$

where $\tau = 2a \exp(\pm\eta)$, and for the potential of the incident SV-wave:

The remaining potentials in (20), by analogy with (23), have the following form:

$$\varphi_2^{(r)} = \sum_{n=0}^{\infty} [C_n H_n^{(1)}(\alpha_2 \tau) + D_n H_n^{(2)}(\alpha_2 \tau)] \cos n\xi e^{-i\omega t}, \quad \psi_2^{(r)} = \sum_{n=0}^{\infty} [E_n H_n^{(1)}(\beta_2 \tau) + F_n H_n^{(2)}(\beta_2 \tau)] \sin n\xi e^{-i\omega t} \quad (24)$$

$$\varphi_3^{(r)} = \sum_{n=0}^{\infty} G_n J_n^{(1)}(\alpha_3 \tau) \cos n\xi e^{-i\omega t}$$

The dynamic stress-strain state is expressed in terms of the potentials φ_1 and ψ_2 :

$$\begin{aligned} u_{\eta i} &= \delta[(\varphi_i)_{\eta} - (\psi_i)_{\xi}] u_{\xi i} = \delta[(\varphi_i)_{\xi} - (\psi_i)_{\eta}], \quad u_{\eta 3} = -\delta(i\omega)^{-1}(\varphi_3) \\ \sigma_{\eta\eta i} &= -\sigma_{\xi\xi i} = 2\delta^2 \{d_i [0,5\varphi_{\eta\eta} - (\varphi_{\xi} + \varphi_{\eta}) \sin \xi] + 0,5\lambda_i \varphi_{\xi\xi} - \mu_i (\psi_{\xi\xi} - \varphi_{\eta} + \psi_{\xi})\} \\ \tau_{\eta\eta 3} &= \sigma_{\xi\xi 3} = -i\omega_3 \rho_3 \varphi_3, \quad \tau_{\eta\xi i} = 2\mu_i \delta^2 [\varphi_{\xi\eta} + 0,5\psi_{\eta\eta} - 0,5\psi_{\xi\xi} + \varphi_{\xi} + \psi_{\eta} + (\varphi_{\xi} - \psi_{\xi}) \sin \xi] \\ i &= 1, 2; \delta = e^{\mp\eta} / 2a. \end{aligned} \quad (25)$$

By substituting (24) and (25) into (8), we obtain the final solutions to the problems of the incidence of P- and SV-waves on two underground pipes, respectively. The arbitrary constants A_n , B_n , C_n and others are determined from a system of algebraic equations with complex coefficients.

$$[C]\{q\}=\{\rho\}$$

where C is a determinant of order 12×12 , whose elements are Bessel and Hankel functions of the first and second kind of order n ; q is the column vector of unknown quantities, and ρ is the right-hand-side vector.

The system of algebraic equations with complex coefficients is solved using the Gauss method with pivot selection. The dynamic stress-strain state in the case of an incident shear wave acting on two underground pipes is also written in bipolar coordinates in an asymptotic form:

$$u_z = w, \sigma_{\eta z} = \mu_i \delta(u_z)_\eta, \sigma_{\xi z} = \mu_i \delta(u_z)_\xi \quad (26)$$

As the boundary conditions, we use condition (23) and the substitution $r = \eta$. The final solution of the problem for the case of an incident SH-wave on two pipes has the following form:

$$\begin{aligned} u_{z1} &= w_0 \sum_{n=0}^{\infty} [\varepsilon_n J_n(k_1 \tau) + A_n H_n^{(1)}(k_1 \tau)] \cos n \xi e^{-i w \tau}; u_{z2} = -w_0 \sum_{n=0}^{\infty} [B_n H_n^{(1)}(k_2 \tau) + C_n H_n^{(2)}(k_2 \tau)] \cos n \xi e^{-i w \tau}; \\ \sigma_{r1} &= \mu_1 w_0 k_1 \sum_{n=0}^{\infty} [\varepsilon_n J_n(k_1 \tau) + A_n H_n^{(1)}(k_1 \tau)] \cos n \xi e^{-i w \tau}; \sigma_{r2} = -\mu_2 w_0 k_2 \sum_{n=0}^{\infty} [B_n H_n^{(1)}(k_2 \tau) + C_n H_n^{(2)}(k_2 \tau)] \cos n \xi e^{-i w \tau}; \\ \sigma_{\theta 1} &= -\mu_1 w_0 n \sum_{n=0}^{\infty} [\varepsilon_n (k_1 \tau) + A_n H_n^{(1)}(k_1 \tau)] \sin n \xi e^{-i w \tau}; \sigma_{\theta 2} = \mu_2 w_0 n \sum_{n=0}^{\infty} [B_n H_n^{(1)}(k_2 \tau) + C_n H_n^{(2)}(k_2 \tau)] \sin n \xi e^{-i w \tau}; \end{aligned} \quad (27)$$

The unknown coefficients A_n, B_n, C_n are determined from the boundary conditions. Let us consider the determination of the dynamic stress - strain state of a cylindrical pipe under the action of harmonic waves.

To solve the stated problem, the addition theorem is used. Addition theorems for cylindrical wave functions were derived in works [4, 5, 6]. Let there be two different polar coordinate systems (r_g, θ_g) and (r_k, θ_k) (Fig. 3), whose polar axes have the same direction. The coordinates of the pole θ_k g-system are R_{kg}, θ_{kg} , such that the following equality holds.

$$Z_g = R_{kg} e^{i \theta_{kg}} + Z_k \quad (28)$$

Then the addition theorem takes the following form:

$$\begin{aligned} b_n(\alpha r_q) e^{i n \theta_q} &= \sum_{p=-\infty}^{\infty} b_{n-p}(\alpha R_{kq}) e^{i(n-p)\theta_{kq}} T_p(\alpha r_k) \exp(i p \theta_k), \quad r_k < R_{kq} \\ b_n(\alpha r_q) e^{i n \theta_q} &= \sum_{p=-\infty}^{\infty} J_{n-p}(\alpha R_{kq}) e^{i(n-p)\theta_{kq}} b_p(\alpha r_k) \exp(i p \theta_k), \quad r_k < R_{kq} \end{aligned} \quad (29)$$

Formula (28) makes it possible to transform the solution of the wave equation (1) from one coordinate system to another. Let us consider the analysis of a long underground multi-line pipeline under seismic excitation within the framework of a plane problem of the dynamic theory of elasticity.

In doing so, we examine the case of stationary diffraction of plane waves by a series of periodically arranged cavities reinforced with rings and containing an ideal compressible fluid inside. The solution to the posed problem will be obtained using the potential method. The boundary conditions are given by (8). The form of the incident potential also remains unchanged.

The potentials of the waves reflected from the pipes, after applying the addition theorem and taking into account the periodicity of the problem, will have the following form:

$$\begin{aligned}\varphi_1^{(r)} &= e^{-i\omega t} \sum_{n=0}^{\infty} [A_n H_n^{(1)}(\alpha_1 r) + S_n J_n(\alpha_1 r)] e^{in(\theta-\gamma)}, \\ \psi_1^{(r)} &= e^{-i\omega t} \sum_{n=0}^{\infty} [B_n H_n^{(1)}(\beta_1 r) + \sigma_n J_n(\beta_1 r)] e^{in(\theta-\gamma)}, \\ S_n &= \sum_{p=0}^{\infty} \sum_{m=1}^{\infty} A_p E_p [e^{im\xi} H_{n-p}^{(1)}(\alpha_1 m\delta) + e^{-im\xi} H_{n-p}^{(1)}(\alpha_1 m\delta)], \\ Q_n &= \sum_{p=0}^{\infty} \sum_{m=1}^{\infty} B_p E_p [e^{im\xi} H_{n-p}^{(1)}(\beta_1 m\delta) + e^{-im\xi} H_{n-p}^{(1)}(\beta_1 m\delta)],\end{aligned}\quad (30)$$

where: $\xi = k\delta \cos \gamma$, δ - is the distance between the centers of the pipes.

The potentials of the refracted waves in the pipes are written in the form

$$\begin{aligned}\varphi_2 &= e^{i(m\xi - w\xi)} \sum_{n=0}^{\infty} E_n [C_n H_n^{(1)}(\alpha_1 r) + D_n H_n^{(2)}(\alpha_2 r)] e^{in(\theta-\gamma)}, \\ \psi_2 &= e^{i(m\xi - w\xi)} \sum_{n=0}^{\infty} E_n [E_n H_n^{(1)}(\beta_1 r) + F_n H_n^{(2)}(\beta_2 r)] e^{in(\theta-\gamma)},\end{aligned}\quad (31)$$

and the velocity potential in the ideal compressible fluid

$$\varphi_3 = e^{i(m\xi - w\xi)} \sum_{n=0}^{\infty} E_n G_n J_n(\alpha_3 r) e^{in(\theta-\gamma)},\quad (32)$$

The unknown coefficients A_n - G_n are determined by substituting (29)-(32) into (8). As a result, an infinite system of linear equations is obtained, which is solved using an approximate reduction method, provided that the following relation is not satisfied

$$k\delta(1 \mp \cos \gamma) = 2\pi n$$

The general description of the program is intended for multi-line pipes in an embankment in the case of seismic waves incident perpendicular to the axis passing through the centers of the pipes.

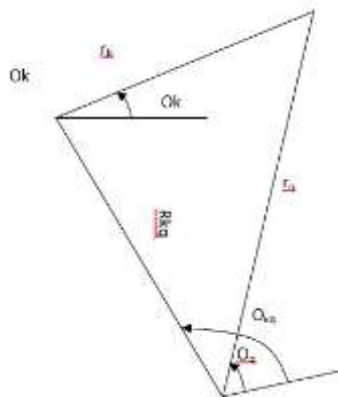


Figure 2. Diagram for the addition theorem.

The input data include the minimum necessary parameters: the elastic properties (E and ν) of the embankment soil and the pipes; the density of the soil, the pipe, and the fluid filling it; the inner and outer radii of the pipes; the predominant period of soil particle oscillation; the coordinates of the point at which the stress–strain state is evaluated; and the seismicity coefficient.

Using a special option, it is possible to perform calculations for pipes filled with an ideal compressible fluid as well as for empty ones. The cylindrical Bessel and Hankel functions are computed using known formulas. The system of linear equations is solved by the Gauss method with pivot selection.

Influence of the distance between the pipes. Table 1 presents the values of the coefficient

$$\eta_{\max} (\eta_{\max} = |\sigma_{rr}| / (\lambda + 2\mu)\alpha^2 A$$

of the maximum radial soil pressure on the pipes for different distances d between them in the case of an incident P-wave. The following parameters were assumed: the P-wave number $\alpha_r = 1.0$; the inner and outer radii of the pipes $R_0 = 0.8$ m and $R = 1.0$ m; the predominant period of soil particle oscillation $T = 0.2$ s. The properties of the embankment soil are: Lamé constants $\lambda_1 = 8.9$ MPa, $\mu_1 = 4.34$ MPa, density $\rho_1 = 1.74$ kN. The properties of the pipe material are: $\lambda_2 = 8690$ MPa, $\mu_2 = 12930$ MPa and density $\rho_2 = 2.55$ kN*s²/m⁴.

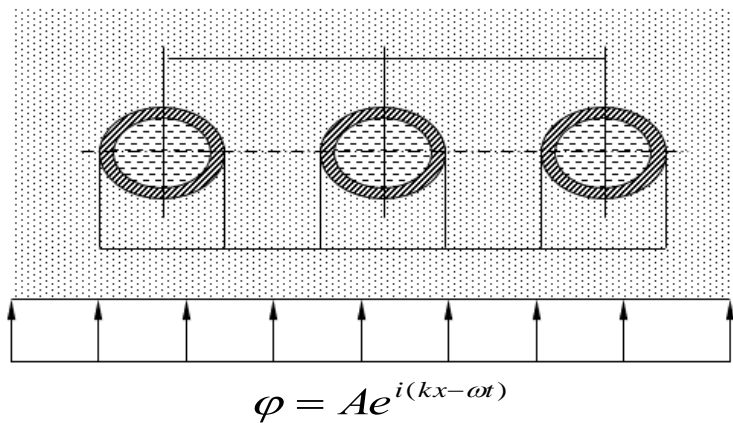


Figure 3. Computational scheme.

Table.1
The value of the dynamic concentration coefficient for different distances between the pipes in the case of an incident P-wave

D/d	0,5	1,0	2,0	4,0
η_{\max}	1,68	1,76	1,61	1,60

From Table 1, it follows that at first, as the distance between the pipes increases within the range $0.5 \leq d / D \leq 1.0$, the coefficient η_{\max} increases slightly-by about 5%. With a further increase of $d / D > 1.0$, it decreases more sharply-by about 10%. When $d / D > 2.0$, the value of η_{\max} stabilizes, i.e., it practically does not change, and for $1 \leq 4.0$ it is close to the η_{\max} value for a single pipe according to the calculations. Therefore, the mutual influence of the reinforced-concrete pipes in a multi-line arrangement is significant when the distance between them satisfies $d \leq 4.0$,

which leads to an increase in the maximum dynamic soil pressure on them compared to a single pipe. This increase in the coefficient η_{\max} is associated with the superposition of waves reflected from several surfaces of the multi-line pipes.

The non-monotonic increase of the coefficient η_{\max} with a decrease in the spacing d / D is, in our opinion, related to the interference of waves superimposed after reflection. This phenomenon is extremely important in the practical design of seismic underground multi-line pipelines, as it allows selecting an optimal spacing between the pipes at which the dynamic pressure under seismic loading is minimal. For example, according to Table 1, such a spacing is $d=0.5D$. It is known, for comparison, that under static loading the opposite trend is observed: the soil pressure on multi-line pipes is lower than on a single pipe. In addition to the above, when analyzing the influence of the distance between pipes on their stress-strain state, one must take into account relation (28) (the so-called “sliding points”), at which a significant increase in dynamic stresses is observed near the pipe-resonance. This phenomenon, known in optics as the Wood anomaly, is a characteristic feature of multi-line pipelines and cannot occur in a single-line pipeline. From the standpoint of design practice, it is necessary to know at what spacing the pipes can be laid so that the dangerous resonance phenomenon does not occur. This question is answered by relation (27). Let us analyze this relation for the case of incident P- and SV-seismic waves acting on the underground pipeline. Table 2 presents the dependence of the maximum clear spacing between the pipe centers d_{\max} , at which resonance does not occur, on the angle of incidence γ of the seismic waves.

Table.2

Dependence of the distance D_{\max} on the angle of incidence γ .

Degree, γ	0	30	45	60	70	80	90
D_{\max} , M	5,0	5,36	5,86	6,66	7,45	8,52	10,0

From Table 2, it follows that the smaller the angle of incidence of the seismic wave on the pipeline, the closer the pipes must be placed to each other. Thus, the occurrence of resonance in multi-line pipelines can be avoided by selecting an appropriate distance between them, thereby ensuring the seismic resistance of the pipeline. Influence of the type of seismic excitation (P-, SV-, or SH-wave).

Table 3 presents the values of η_{\max} - the maximum radial soil pressure on the pipes - for the incidence of P- and SV-type seismic waves at various distances d between the pipes. In this case, $\beta_r = 2$ was assumed. Analysis of the data in Table 3 shows that for $d/D < 4,0$ the values of the coefficient η_{\max} for P- and SV-waves are essentially in opposite phases. That is, at $d/D = 1,0$, the maximum seismic impact of the P-wave is 27% higher than that of the SV-wave, at $d/D = 2,0$ it is 7% lower, and at $d/D = 4,0$ it becomes higher again, but only by about 1%. As the distance between the pipes increases, the difference between these impacts decreases, and at $d/D = 4,0$ it practically disappears altogether. In addition, it should be noted that under SV-wave excitation, the values of η_{\max} for different distances between the pipes exhibit a scatter 2.5 times larger (up to 25%) compared to P-wave excitation (up to 10%). Thus, the phenomenon of “local resonance” is more strongly pronounced for seismic excitation in the form of an SV-wave.

Table.3

Values of the coefficient η_{\max} under seismic excitation in the form of P- and SV-waves at various distances d between the pipes

d/D	η_{\max}	
	P-wave	SV- wave
1,0	1,76	1,29
2,0	1,61	1,72
4,0	1,60	1,51

Table 4 presents the values of the coefficient η_{\max} for the incidence of a P-wave on empty and water-filled pipes at various distances d between the pipes. The density of the fluid was taken as $\rho_3 = 0.102 \text{ kN} \cdot \text{s}^2/\text{m}^4$.

Table.4

Values of the coefficient η_{\max} for the incidence of a P-wave on empty and water-filled pipes

d/D	η_{\max}	
	P-wave	SV- wave
1,0	1,76	1,89
2,0	1,61	1,78
4,0	1,60	1,90

From Table 4, it follows that the presence of water in the pipes increases the seismic effects on them compared to empty pipes. This is obviously related to the increase in the mass of the pipeline. The maximum dynamic soil pressure on the pipes becomes stronger. For example, at $d/D = 1.0$ the difference in the coefficient values is: at $d/D = 2,0$ - 10%, at $d/D = 4,0$ - 19%.

In addition, it should be noted that the variation in the values of the coefficient η_{\max} at different distances d for water-filled pipes is smaller (7%) than for empty pipes (10%).

Table 4 presents the values of the coefficient η_{\max} for various wavelengths $l_0/l_0-2\pi/\alpha$ of a P-wave incident on empty pipes placed at a distance of $l = 1,0 D$ from each other.

Table.5

Values of the coefficient η_{\max} for various wavelengths l_0 of the P-wave.

l_0/D	3,0	5,0	10,0
η_{\max}	1,76	1,52	1,20

From Table 5, it follows that the greater the wavelength of the incident seismic wave-that is, the denser the embankment soil-the smaller the coefficient η_{\max} becomes. For reference, note that the ratio $l_0 / D = 5.0$ corresponds to loose sandy, sandy-loam, and loamy soils, while $l_0 / D = 10.0$ corresponds to clayey soils. Thus, the type of soil, and especially its density, has a significant influence on the dynamic pressure exerted on the pipes under seismic loading. Hence, when constructing an embankment over the pipes, it is necessary to thoroughly compact the fill soil.

It is interesting to note that good compaction of the soil also reduces its static pressure on the pipes. In addition, calculations show that when $l_0 > 10.0 D$, the dynamic problem reduces to a quasi-static one, which significantly simplifies its solution. From this, an important conclusion follows: the quasi-static approach is not applicable for evaluating the seismic impact on pipes located beneath embankments.

Influence of the pipe wall thickness. Table 6 presents the values of the coefficient η_{\max} for various wall thicknesses t of a reinforced-concrete pipe in the case of a P-wave incident on empty multi-line pipes laid at a distance of $d = 0,5$.

Table.6

Values of the coefficient η_{\max} for different pipe wall thicknesses t .

d/D	0,08	0,1	0,15	0,2
η_{\max}	1,60	1,66	1,66	1,68

From Table 6, it follows that the range of wall thicknesses has practically no influence on the dynamic soil pressure on these pipes. This is apparently due to the fact that the harmonic wave does not penetrate into the reinforced-concrete pipe because of its sufficient rigidity.

Conclusions.

1. Under seismic loading, the mutual influence of reinforced-concrete pipes in multi-line arrangements occurs when the distance between them is $d > 4,0D$ and leads to an increase in the maximum dynamic soil pressure on them, compared to a single pipe (the phenomenon of local resonance), by 5–10%.
 2. The occurrence of resonance in multi-line pipelines can be avoided by selecting distances between the pipes that are not multiples of the wavelength of the incident seismic wave. This resonance phenomenon is a characteristic feature of multi-line pipelines and cannot occur in a pipeline laid in a single line.
 3. The phenomenon of local resonance is more strongly pronounced under seismic excitation in the form of an SV-wave than in the form of a P-wave.
 4. The presence of water in the pipes increases the seismic impact on them by 10–20%.
 5. The denser the embankment soil, the smaller the seismic impact on underground pipes. When $l > 10D$, the dynamic problem reduces to a quasi-static one.
 6. Changes in wall thickness and concrete grade have virtually no effect on the dynamic soil pressure on reinforced-concrete pipes under seismic loading.
- Similar dependencies were also obtained for the case $\gamma=0$. It is interesting to note that, in the problem under consideration, the increase in stress concentration caused by the proximity of another discontinuity region is much greater when the wave approaches from the side (i.e., $\gamma=0$) than when the wave approaches from above (i.e., $\gamma=\pi/2$).
7. The maximum dynamic soil pressure σ_{\max} on pipes laid in two lines at a distance of $d < 3,0 D$ from each other is greater than that on a single pipe. This increase reaches up to 15%.
 8. The presence of fluid in the pipes generally increases the pressure σ_{\max} by about 20% for a single pipe and by 5–10% for two-line pipe systems. An exception is tightly packed pipes with $d=0$, for which the pressure σ_{\max} decreases by 4%.

Literature

1. Gazetas, G. Soil–Structure Interaction: Foundation Vibrations. Soil Dynamics and Earthquake Engineering, 1991.
2. Achenbach, J. D. Wave Propagation in Elastic Solids. North-Holland, 1973.
3. Kuznetsov, V. D. Seismic Resistance of Underground Structures. Moscow: MIR Publishers, 1986.
4. Novak, M. Soil–Structure Interaction Under Dynamic Loads. Earthquake Engineering and Structural Dynamics, 1974.
5. Kausel, E. Fundamentals of Earthquake Engineering. Cambridge University Press, 2010.
6. Yeh, C.-H., Yang, J. N. Response of Buried Pipelines to Seismic Excitation. Journal of Pressure Vessel Technology, 1984.
7. O'Rourke, M. J., Liu, X. Seismic Design of Buried and Offshore Pipelines. MCEER Monograph, 1999.
8. Takemiya, H. Dynamic Soil–Structure Interaction for Underground Lifelines. Soil Dynamics Symposium, 1985.
9. Shukla, S. K., Yin, J.-H. Fundamentals of Soil Mechanics. CRC Press, 2006.
10. Abousleiman, Y., Cheng, A. H.-D. Poromechanics and Wave Diffraction in Saturated Media. ASCE, 2013.
11. Aitaliev, Zh. M., Yerzhanov, N. S. Seismic Stresses of Underground Structures in Anisotropic Medium. Nauka, 1980.
12. Timoshenko, S., Goodier, J. N. Theory of Elasticity. McGraw-Hill, 1970.
13. Zienkiewicz, O. C., Taylor, R. Finite Element Method in Dynamics. McGraw-Hill, 1991.
14. Gorshkov, A. G. *Dynamic Interaction of Shells and Plates with the Surrounding Medium*. Moscow: Academy of Sciences Publishing, Solid Mechanics, No. 2, 1976, pp. 165–178.
15. Guz, A. N., Golovchin, V. T. *Diffraction of Elastic Waves in Multiply-Connected Bodies*. Kiev: Naukova Dumka, 1972, 254 p.
16. Rashidov, T. R. *Dynamic Theory of Seismic Resistance of Complex Systems of Underground Structures*. Tashkent: Fan Publishing, 1973, 182 p.
17. Yerzhanov, N. S., Aitaliev, Zh. M., Masanov, Zh. K. *Seismic Stress State of Underground Structures in an Anisotropic Medium*. Alma-Ata: Nauka, 1980, 211 p.
18. Muborakov, Ya. N. *Seismic Dynamics of Underground Shell-Type Structures*. Tashkent: Fan, 1987, 192 p.
19. Pao, Y. H., Mow, C. C. *The Diffraction of Elastic Waves and Dynamic Stress Concentrations*. New York: Crane Russak & Co., 1973, 694 p.
20. Avliyakov, N. N., Safarov, I. I. *Modern Problems of Statics and Dynamics of Underground Pipelines*. Tashkent: Fan va Texnologiya, 2007, 306 p.
21. Safarov, U., Ishmamatov, M., Kulmurov, N., Xalilov, S., & Axmedov, N. (2022). Vibration of buried pipes insulated with soft soil under exposure to seismic loads. *AIP Conference Proceedings*, 2432, 1–6. <https://doi.org/10.1063/5.0091544>
22. Safarov, U., Axmedov, S., Tursunov, I., Boltayev, S., & Xakimov, S. (2022). Natural vibrations of reinforced viscoelastic cylindrical shells with a viscoelastic filler. Part 1. *AIP Conference Proceedings*, 2432, 1–5. <https://doi.org/10.1063/5.0117821>

23. Safarov, U., Axmedov, S., Kulmuratov, N., Choriyev, M., & Hamrayev, N. (2021). Vibrations of deformable cylindrical shells with a viscoelastic filler. *Theoretical & Applied Science*, 101(9), 178–186.
24. Safarov, U., Teshayev, M., Djurayev, S., & Eshpo'latov, B. (2022). Non-story vibration of a viscoelastic cylindrical shell with a viscous fluid. *International Journal of Innovative Analyses and Emerging Technology*, 2(1), 63–70.
25. Safarov, U., & Isroilov, B. E. (2025). Investigation of the interaction of tunnel structures with ground masses under the influence of dynamic loads. *Journal of Multidisciplinary Sciences and Innovations*, 4(3), 532–537. <https://ijmri.de/index.php/jmsi/article/view/465>
26. Safarov, U., & Jumayev, Sh. B. (2025). Seysmik to'liqinni ko'p qatlamli silindrik qobiqqa yuklanishi masalasini yechish metodikasi va algoritmi. *Arxitektura, qurilish va dizayn*, (3), 1066–1071. <https://www.taqu.uz>
27. Safarov, U. I., & Zohidova, Sh. I. (2025). Seysmik to'liqinni ko'p qatlamli silindrik qobiqqa yuklanishi masalasini qo'yilishi va asosiy munosabatlar. *Arxitektura, qurilish va dizayn*, (3), 1078–1081. <https://www.taqu.uz>
28. Safarov, U. I., & Jo'rayev, O'. Sh. (2025). Seysmik to'liqlarning ko'p qatlamli silindrik qobiqqa yuklanishi masalasini qo'yilishi. *Arxitektura, qurilish va dizayn*, (1), 227–234. <https://www.taqu.uz>
29. Сафаров, У. И., Хожиев, А. Х., & Болтаев, З. И. (2025). Воздействие сейсмических волн на подземные многослойные трубопроводы, расположенные в вязкоупругой среде. *Экономика и социум*. https://www.iupr.ru/_files/ugd/b06fdc_ad97d7539af64602aafb2e3bc7050b9c.pdf?index=true
30. Fayzieva, F. A. (2020). The problem of seismic stability of unique historical monuments – The primary problem before us. *Актуальные проблемы гуманитарных и естественных наук. Журнал научных публикаций*, (07), 104–107. <https://www.publikacia.net>
31. Ташмухамедова, Ф. А., & Умарова, З. С. (2024). Анализ и последствия разрушительного землетрясения в Японии. *International Scientific Journal of Modern Science and Research*, 3, 1351–1354. <https://doi.org/10.5281/zenodo.11100380>
32. Fayzieva, F. A., & Jabbarova, X. K. (2020). Cultural heritage is one of the main ways of culture. *International Multidisciplinary Research Journal*, 10, 182–187. <https://saarj.com>
33. Файзиева, Ф. А. (2020). Памятники архитектуры — наше национальное богатство. *Актуальные проблемы гуманитарных и естественных наук. Журнал научных публикаций*, (07), 107–111. <https://www.publikacia.net>